

# Integration Reinforcement of Renewable Energy Resources and PHEVs through Hybrid AC-DC Local Network

Payam Teimourzadeh Baboli<sup>1</sup>, Salah Bahramara<sup>2</sup>, Mohsen Parsa Moghaddam<sup>3</sup>, Mahmoud Reza Haghifam<sup>4</sup>

Received: 2015/5/23 Accepted: 2015/11/28

## Abstract

The share of DC-based Renewable Energy Resources (RERs) and electricity storage systems are increasing due to developments of smart grid technologies. Moreover, the share of DC-based load has rapid growth due to significant developments of power electronic technologies. Therefore, a more flexible power system is required for efficient integration of emerging loads and generators. In this paper, hybrid AC-DC Local Network (LN) is incorporated as an appropriate topology versus conventional AC LN to reinforce the integration of RERs and Plug-in Hybrid Electric Vehicles (PHEVs). A mixed integer linear model is developed for operation of both hybrid AC-DC LN and conventional AC LN topologies considering high penetration of RERs and PHEVs. This operation model is solved by GAMS optimization software to minimize the operation cost and find the optimum inter-resource scheduling in the day-ahead market. Moreover, investment analysis and reliability assessment are carried out for the mentioned LNs. Numerical study is conducted to evaluate the ability of both topologies for better utilizing the opportunities of integration.

**Keywords:** Conventional AC local network, energy efficiency, hybrid AC-DC local network, renewable energy resource, plug-in hybrid electric vehicle.

## Nomenclature

### Indices:

|     |                                   |
|-----|-----------------------------------|
| $c$ | index of load point               |
| $i$ | index of contingency              |
| $k$ | index of PHEVs' discharging steps |

|                          |                                                                            |
|--------------------------|----------------------------------------------------------------------------|
| $m$                      | index of year                                                              |
| $n$                      | index of PHEVs' number                                                     |
| $t$                      | index of hour                                                              |
| <i>Parameters:</i>       |                                                                            |
| $A$                      | annualized cost                                                            |
| $ACIT_i$                 | average customer interruption frequency at load point $i$                  |
| $C_{O\&M}$               | operation and maintenance cost of DG ( $USD$ )                             |
| $frac_{i,k}$             | fraction of the load which is lost at load point $i$ , for contingency $c$ |
| $HR$                     | heat rate ( $kWh/m^3$ )                                                    |
| $i_R$                    | annual real interest rate (%)                                              |
| $Load_{AC}(t)$           | AC load at $t$ ( $kW$ )                                                    |
| $Load_{DC}(t)$           | DC load at $t$ ( $kW$ )                                                    |
| $Load_{Total}(t)$        | total load at $t$ ( $kW$ )                                                 |
| $LPENS_i$                | energy not supplied of the load point $i$                                  |
| $P$                      | present value                                                              |
| $PR_{fuel}$              | fuel price ( $USD$ )                                                       |
| $PR_{sell}$              | electricity selling price to grid ( $$/kWh$ )                              |
| $PR_{TOU}(t)$            | time-of-use rates at $t$ ( $$/kWh$ )                                       |
| $P_{PV}(t)$              | generation of PV panel at $t$ ( $kW$ )                                     |
| $P_{WT}(t)$              | generation of wind turbine at $t$ ( $kW$ )                                 |
| $Pd_i$                   | weighted average amount of power disconnected                              |
| $Pr_c$                   | probability of occurrence of contingency $c$                               |
| $Ps_i$                   | weighted average amount of power shed at load point $i$                    |
| $P_{conv}$               | rated power of converter ( $kW$ )                                          |
| $PEV^{n,charge,max}$     | maximum charging power of $n$ -th PHEV's battery ( $kW$ )                  |
| $PEV^{n,dcharge,max}$    | maximum discharging power of $n$ -th PHEV's battery ( $kW$ )               |
| $P_{DG,max}$             | maximum capacity of DG ( $kW$ )                                            |
| $PG_{max}$               | maximum transmitted power through grid ( $kW$ )                            |
| $RR$                     | ramp rate ( $kW/h$ )                                                       |
| $SOC^{n,min}$            | minimum state-of-charge of $n$ -th PHEV's battery                          |
| $SOC^n(t^{n, arr})$      | state-of-charge of $n$ -th PHEV's battery at arriving time                 |
| $SOC^n(t^{n, dep})$      | state-of-charge of $n$ -th PHEV's battery at departure time                |
| $SOC^n_{in}$             | input state-of-charge of $n$ -th PHEV's battery                            |
| $SOC^n_{out}$            | output state-of-charge of $n$ -th PHEV's battery                           |
| $QEV^n$                  | capacity of $n$ -th PHEV's battery ( $kWh$ )                               |
| $\alpha^k_{dcharge}$     | The coefficient of PHEVs' discharging steps                                |
| $\eta_{AC/DC}$           | efficiency of rectifier (P.U.)                                             |
| $\eta_{DC/AC}$           | efficiency of inverter (P.U.)                                              |
| $\eta_{DG}$              | efficiency of DG unit (P.U.)                                               |
| <i>Binary Variables:</i> |                                                                            |
| $X_{AC/DC}(t)$           | 1 for converted power from AC to DC                                        |

1. PhD student, Email: [pteimourzadeh@ieee.org](mailto:pteimourzadeh@ieee.org)

2. PhD student, Email: [s.bahramara@modares.ac.ir](mailto:s.bahramara@modares.ac.ir)

3. Professor, corresponding author, [parsa@modares.ac.ir](mailto:parsa@modares.ac.ir),

4. Professor, Email: [Haghifam@modares.ac.ir](mailto:Haghifam@modares.ac.ir)

|                            |                                                                   |
|----------------------------|-------------------------------------------------------------------|
|                            | at $t$ , 0 otherwise                                              |
| $X_{DC/AC}(t)$             | 1 for converted power from DC to AC at $t$ , 0 otherwise          |
| $X^n_{charge}(t)$          | 1 for $n$ -th PHEV's battery charging at $t$ , 0 otherwise        |
| $X^n_{discharge}(t)$       | 1 for $n$ -th PHEV's battery discharging at $t$ , 0 otherwise     |
| $XG_{in}(t)$               | 1 for power purchase from grid at $t$ , 0 otherwise               |
| $XG_{out}(t)$              | 1 for power sells to grid at $t$ , 0 otherwise                    |
| Variables:                 |                                                                   |
| $F(t)$                     | consumption of natural gas at $t$ ( $m^3$ )                       |
| $P_{AC/DC}(t)$             | converted AC to DC power at $t$ ( $kW$ )                          |
| $PEV^n_{charge}(t)$        | charging power of $n$ -th PHEV's battery at $t$ ( $kW$ )          |
| $PEV^{n,k}_{discharge}(t)$ | discharging power steps of $n$ -th PHEV's battery at $t$ ( $kW$ ) |
| $PEV^n_{discharge}(t)$     | discharging power of $n$ -th PHEV's battery at $t$ ( $kW$ )       |
| $P_{DC/AC}(t)$             | converted power from DC to AC at $t$ ( $kW$ )                     |
| $P_{DG}(t)$                | generation of DG at $t$ ( $kW$ )                                  |
| $PG_{in}(t)$               | purchased power from external grid at $t$ ( $kW$ )                |
| $PG_{out}(t)$              | delivered power to external grid at $t$ ( $kW$ )                  |
| $SOC^n(t)$                 | state-of-charge of battery at $t$ (P.U.)                          |

## 1. Introduction

Widespread use of Renewable Energy Resources (RERs) in low voltage AC distribution networks is endorsed due to environmental, customers' security and grid's efficiency issues. New small generators with intermittent output power are entered in the distribution network. AC microgrids facilitate the connection of the mentioned resources with conventional AC distribution systems. Thus, the nature of generation portfolio is changing. Besides, load's observability and controllability are increased by developing smart grid technologies. Moreover, penetration of storage systems is also increasing in distribution level, e.g. batteries and plug-in hybrid electric vehicles (PHEVs). In such environment, strong integration of RERs and PHEVs is one of the main goals of power system planners. In this paper, inclusion of DC link is suggested as an appropriate solution for reinforcing the integration of the mentioned demand-side resources.

Most low-voltage resources produce DC power which has to be converted into AC, by DC/DC converters and be inverted to AC, in order to be

connected to the conventional AC grid. Meanwhile, DC loads such as inverter-based home appliances (e.g. TV, computer, stove, dishwasher, etc.), light-emitting diode (LED) lights and electric vehicles are connected to the AC power system through AC/DC and DC/DC converters. Recently, DC microgrids are resurging due to the increasing penetration of DC power resources and loads [1, 2]. Conversely, in DC microgrids, the generated power of AC-based resources have to be converted into DC before connecting to the DC link and DC/AC inverters are required for servicing conventional AC loads. It can be concluded that, multiple reverse conversions are required in each AC or DC microgrids which may add additional operation and investment costs and losses to the system [3]. Thus, it can be figured out that employment of hybrid AC-DC microgrids will be underlined in the future perspective of distribution systems.

PHEVs provide several advantages for owners which lead to their increasing share in future transportation system. Moreover, their storages ability facilitates the integration of RERs into distribution network that is the most transformative impact on the power system. The literatures on this topic are mainly concentrated on investigation of wind and solar energy [4-9]. Besides, the concept of hybrid microgrid has been investigated as an economical, environmental friendly and efficient distribution grid of the future from different viewpoints [10-14]. Liu *et al* applied a centralized coordination control algorithm for smooth power transfer between AC and DC links [10, 11]. Although the controllability and predictability of centralized control methods are high in compare with decentralized control methods, the promptness and reliability of them are much fewer. Therefore, a system control failure may lead to total grid outage. A dynamic assessment of hybrid AC-DC system is investigated in Ref. [12]. Authors in [13] employed power consumption control with the droop characteristic and maintained the DC bus voltage within the acceptable range. In the latter study, the test system was consisted of a wind generator and several controllable loads with no controllable generators, e.g. DG unit, fuel cell, etc. Moreover, Ref. [13] did not investigate the stand-alone operation in contingency states. These studies are focused on power electronic aspects of the problem or the control framework of the system in a constant operating point.

This paper investigates the optimum operation of hybrid AC-DC Local Network (LN) considering the time-dependence impacts of the network over 24 hours. Here, two different microgrid configurations are considered with the same amount of electricity consumption and local generation. Indeed, the important role of grid's configuration is investigated in this study. In the first configuration (conventional AC LN), there are three kinds of small-scale RERs (i.e. wind turbine, photovoltaic arrays and distributed generator), several PHEVs and the electricity load. All of them are connected to an AC distribution network and the extra/shortage of power is transmitted with the external grid. The second configuration (the proposed hybrid AC-DC LN) is consisted of all the mentioned resources and load with similar quantity. But, there is semi-separated AC and DC links that reinforces the integration of RERs and PHEVs to reduce the intermittency problem of RERs. Regarding this matter, the operation frameworks of both configurations are modeled. The optimum solution of both configurations is compared with each other and the amount of efficiency improvement is demonstrated. In addition to the operation cost comparison, an investment analysis is conducted for providing better economical evaluation of the LNs. Reliability assessment is carried out to compare the technical issues of the LNs. Within the above context, the contributions of the paper are twofold:

- 1) A mixed integer linear model for comparing the operation of hybrid AC-DC and conventional AC LNs are proposed considering the RERs and PHEVs to underline the impacts of the distribution network topology on the integration of RERs and PHEVs.
- 2) In addition to conducting economic evaluation of both LNs by running the cost-benefit analysis in the operation and investment time-scales, a technical comparison is carried out by running the reliability assessment of the mentioned LNs.

The reminder of the paper is organized as follows. Section 2 describes the topologies of both conventional AC and hybrid AC-DC LNs. In section 3, the mathematical formulation of both mentioned topologies is presented. Section 4 presents the numerical results of a case study. Finally, section 5 concludes the paper.

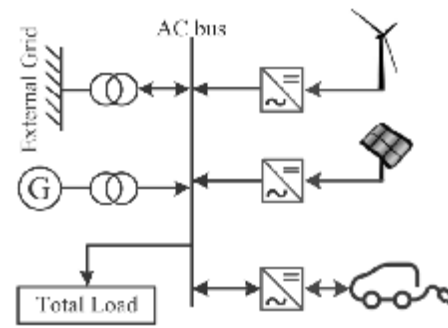


Fig. 1. Conventional AC LN.

## 2. Topology Description

In this section, two different topologies are presented in details to model conventional AC and hybrid AC-DC LNs.

### 2.1. Conventional AC Local Network

The configuration of the AC LN is shown in Fig. 1. This LN is consisted of AC lines (buses), fossil-fuel-based generator (micro-turbine), RERs (wind turbine and photovoltaic arrays) and storage system (PHEVs) which serves an AC load. The power balance of the network is provided by power transactions with external grid.

### 2.2. Hybrid AC-DC Local Network

Hybrid AC-DC LN is proposed to reduce losses of multiple power conversions and to facilitate the connection of various AC and DC resources and loads. Operation problem of a hybrid LN is more complicated than conventional AC LNs. Fig. 2 illustrates the proposed hybrid AC-DC LN topology which has the following advantages:

- 1) When AC link experiences contingency conditions, the DC link can be disconnected from the failure section and continues supplying DC loads. However, most highly power dependent loads such as digital grade loads are DC loads.
- 2) Each DC generator can be deployed easily because it controls only the DC bus voltage.
- 3) The cost and loss of DC sub-system can be reduced because many power electronic converters are omitted from both DC resource units and end-use appliances and equipments.
- 4) Some RERs inherently generate DC power. Therefore, the total cost and loss of the system can be reduced considerably. Regarding this matter,

developing hybrid AC-DC LN enables high penetration of RERs, especially when they are integrated with PHEVs.

5) Although developing the DC sub-system has high investment cost, the total operation cost of the hybrid AC-DC LN is satisfactory.

As shown in Fig. 2, in the hybrid LN, both DC and AC resources are incorporated in power generation. The main electricity power is injected from sub-transmission substation (external grid) to balance AC

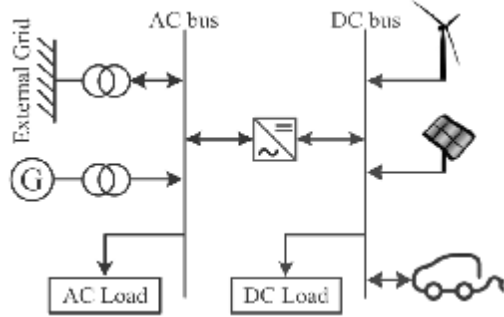


Fig. 2. Hybrid AC-DC LN.

of the main converter between AC and DC links.

### 3. Mathematical formulation

In the following, the mathematical formulation of both conventional AC and hybrid AC-DC LN topologies are presented. The objective function is minimizing the overall operation cost over the entire scheduling period. The supply quantity of RERs are forecasted and considered as input data. Regarding this matter, the scheduling problem is to determine the supply quantity of DG unit, charge/discharge rate of the PHEVs and the amount of power transactions with external grid over 24 hours as formulated in the following:

$$OC = \sum_{t=1}^{24} \left[ \begin{array}{l} PG_{in}(t) \times PR_{TOU}(t) \\ -PG_{out}(t) \times PR_{sell} \\ + \{ F(t) \times PR_{fuel} + C_{O\&M} \} \\ + \sum_{n=1}^{10} \left( \sum_{k=1}^3 PEV_{dcharge}^{n,k}(t) \times PR_{TOU}(t) \times a_{dcharge}^k \right) \\ - \sum_{n=1}^{10} PEV_{charge}^n(t) \times PR_{TOU}(t) \end{array} \right] \quad (1)$$

The first term of Eq. (1) determines the energy purchase cost from external grid when the total generation of LN resources is not adequate for serving its load. The second term represents the income from selling the extra amount of LN's generation to the

external grid. The third term demonstrates the operation cost of DG unit that consists of fixed operating and maintenance costs and variable cost related to the consumption and price of the fuel. The fourth term denotes the total cost of all PHEVs that consist of the cost of discharging the battery of PHEVs and the income from charging them. As it is indicated in Eq. (1), three charging steps is considered for discharging the batteries of PHEVs.

The constraints of both LN topologies are formulated as follows:

#### 3.1. Conventional AC LN constraints:

a) Power balance equation:

$$h_{DC/AC} \left( P_{WT}(t) + P_{PV}(t) + \sum_{n=1}^N \sum_{k=1}^3 PEV_{dcharge}^{n,k}(t) \right) + P_{DG}(t) + PG_{in}(t) = Load_{Total}(t) + \left( \sum_{n=1}^N PEV_{charge}^n(t) \right) + PG_{out}(t) \quad (2)$$

where  $Load_{Total}(t)$  is calculated by Eq. (3):

$$Load_{Total}(t) = Load_{AC}(t) + \frac{Load_{DC}(t)}{h_{AC/DC}} \quad (3)$$

The consumption of DC loads is measured while they are connected to the DC link. Thus, when these loads are supplied by AC voltage the rectifier's loss must be considered as it is indicated in Eq. (3).

b) Constraint of DG unit operation:

- Constraint of maximum and minimum power of DG:

$$0 \leq P_{DG}(t) \leq P_{DG,max} \quad (4)$$

- Constraint of ramp rates of DG:

$$0 \leq P_{DG}(t) - P_{DG}(t+1) \leq RR \quad (5)$$

$$0 \leq P_{DG}(t+1) - P_{DG}(t) \leq RR \quad (6)$$

- Output power of DG unit:

$$P_{DG}(t) = F(t) \times HR \times h_{DG} \quad (7)$$

c) Constraint of PHEVs:

- Maximum charge/discharge rate constraint of the PHEVs:

$$0 \leq PEV_{charge}^n(t) \leq X_{charge}^n(t) \times PEV_{charge,max}^n \quad (8)$$

$$0 \leq PEV_{dcharge}^n(t) \leq X_{dcharge}^n(t) \times PEV_{dcharge,max}^n \quad (9)$$

where  $PEV_{dch\ arg e}^n(t)$  is calculated as following:

$$PEV_{dch\ arg e}^n(t) = \sum_{k=1}^3 PEV_{dch\ arg e}^{n,k}(t). \quad (10)$$

As it is indicated in Eq. (10) three discharge steps are considered based on the State-of-Charge (SOC) of the PHEVs' batteries. This kind of modeling increases the fairness of paying the remuneration schemes and prevents unnecessary deterioration of PHEV's battery.

Equation (11) determines the operation mode of the battery by defining two binary variables. By implying this constraint simultaneous occurrence of charging and discharging mode is prevented when the vehicle is in the parking. Moreover, it prevents any charging/discharging power of the PHEV's battery before arriving to or after departing from the parking.

$$\begin{cases} X_{ch\ arg e}^n(t) + X_{dch\ arg e}^n(t) \leq 1 & , \quad t_{arr}^n \leq t \leq t_{dep}^n \\ X_{ch\ arg e}^n(t) = X_{dch\ arg e}^n(t) = 0 & , \quad otherwise \end{cases} \quad (11)$$

- Constraint of discharging steps:

Constraint (12) depicts the limitation of the first discharging step and controls the discharging power of step 1 when  $0.7 \leq SOC^n(t) \leq 1$ .

$$0 \leq PEV_{dch\ arg e}^{n,1}(t) \leq (SOC^n(t) - 0.7) \times QEV^n \quad (12)$$

Constraint (13) depicts the limitation of the second discharging step and controls the discharging power of step 2 when  $0.4 \leq SOC^n(t) < 0.7$ .

$$\begin{cases} 0 \leq PEV_{dch\ arg e}^{n,2}(t) \leq (SOC^n(t) - 0.4) \times QEV^n \\ 0 \leq PEV_{dch\ arg e}^{n,2}(t) \leq (0.7 - 0.4) \times QEV^n \end{cases} \quad (13)$$

Constraint (14) depicts the limitation of the third discharging step and controls the discharging power of step 3 when  $0.2 \leq SOC^n(t) < 0.4$ .

$$\begin{cases} 0 \leq PEV_{dch\ arg e}^{n,3}(t) \leq (SOC^n(t) - 0.2) \times QEV^n \\ 0 \leq PEV_{dch\ arg e}^{n,3}(t) \leq (0.4 - 0.2) \times QEV^n \end{cases} \quad (14)$$

- Constraint of SOC:

The SOC of PHEV's battery constraint is formulated in (15). As it is shown in Eq. (16), the amount of SOC in each time step depends on SOC of pervious time step, charge/discharge power of the battery in pervious time step and its nominal capacity.

$$SOC_{min}^n \leq SOC^n(t) \leq 1 \quad (15)$$

$$SOC^n(t+1) = SOC^n(t) + \frac{PEV_{ch\ arg e}^n(t) - PEV_{dch\ arg e}^n(t)}{QEV^n} \quad (16)$$

Equations (17) and (18) fix the amount of PHEV's SOC in the arrival to and departure time from the parking, respectively.

$$SOC^n(t_{arr}^n) = SOC_{in}^n \quad (17)$$

$$SOC^n(t_{dep}^n) = SOC_{out}^n \quad (18)$$

d) *Constraint of trading with the grid:*

Equations (19)-(21) address the constraints of bidirectional power transmission between LN and external grid.

$$0 \leq PG_{in}(t) \leq X_{in}(t) \times PG_{max} \quad (19)$$

$$0 \leq PG_{out}(t) \leq X_{out}(t) \times PG_{max} \quad (20)$$

$$X_{in}(t) + X_{out}(t) \leq 1 \quad (21)$$

### 3.2. Hybrid AC-DC LN constraints:

Unlike conventional AC LN, there are two power balance equations in hybrid AC-DC LN both in AC and DC buses.

a) *Power balance at AC bus:*

$$\begin{aligned} P_{DG}(t) + PG_{in}(t) + (P_{DC/AC}(t) \times h_{DC/AC}) \\ = Load_{AC}(t) + PG_{out}(t) + P_{AC/DC}(t) \end{aligned} \quad (22)$$

b) *Power balance at DC bus:*

$$\begin{aligned} P_{WT}(t) + P_{PV}(t) + \sum_{n=1}^N \sum_{k=1}^3 PEV_{dch\ arg e}^{n,k}(t) \\ + (P_{AC/DC}(t) \times h_{AC/DC}) = Load_{DC}(t) \\ + \left( \sum_{n=1}^N PEV_{ch\ arg e}^n(t) \right) + P_{DC/AC}(t) \end{aligned} \quad (23)$$

c) *Constraint of converter:*

As described in the section 2, the role of converter is to perform the power balance in DC link. Thus, it has a critical role in operation problem optimization of the system and the results are so sensitive regarding variation of its characteristics e.g. converter's capacity and its conversion efficiency. Equations (24)-(26) present the constraints of the mentioned converter.

$$P_{AC/DC}(t) \leq X_{AC/DC}(t) \times P_{conv} \quad (24)$$

$$P_{DC/AC}(t) \leq X_{DC/AC}(t) \times P_{conv} \quad (25)$$

$$X_{AC/DC}(t) + X_{DC/AC}(t) \leq 1 \quad (26)$$

d) *Other constraints*

Additional constraints (4)-(21) of conventional AC LN are valid for the hybrid AC-DC LN.

#### 4. Reliability Assessment

Since, maintaining the reliability of the network is a crucial issue for both operators and planners of the system, a reliability-wise comparison is done between hybrid AC-DC and AC conventional LNs. Regarding this matter, the expected energy not supplied (EENS) and average service index (ASUI) are chosen to indicate the reliability level of both LNs.

The network reliability assessment produces two sets of indices; i.e. *load point* and *system* indices. Load point indices are calculated for each individual load point. Many system indices are calculated from these load point indices. This section gives the principle equations for calculating EENS and ASUI indices. Firstly, the average customer interruption frequency (ACIT) is calculated by (27).

$$ACIT_i = \sum_c Pr_c \times frac_{i,c} \quad (27)$$

For unsupplied loads, or for loads that are shed completely,  $frac_{i,k}=1$ . For loads that are shed only partly,  $0 < frac_{i,k} < 1$ . Equation (28) presents the load point energy not supplied (LPENS) which is required for calculating EENS.

$$LPENS_i = ACIT_i \times (Pd_i + Ps_i) \quad (28)$$

$$EENS = \sum_i LPENS_i \quad (29)$$

ASUI is the probability of having one or more loads interrupted in the system and is computed as follows:

$$ASUI = \frac{\sum_i ACIT_i \times C_i}{8760 \times \sum_i C_i} \quad (30)$$

#### 5. Numerical Study

In this section, the case study is presented and the results are discussed.

##### 5.1. System Description and Specification

In this study, a four-story university building [15], is considered as the case study to evaluate the effectiveness of the proposed methodology. The main electrical equipments of the building are as follows: air-conditioning, lighting, computers and laboratory appliances. Both AC and DC parts of the electricity load of the proposed system are illustrated in Fig. 3.

The lighting system makes the main part of the electricity consumption from 22:00 to 6:00. As indicated in Fig. 3, the share of DC loads in the mentioned period is at the minimum level over the whole day. While, in the working hour period of the faculty the share of DC load is increased up to 50 percent.

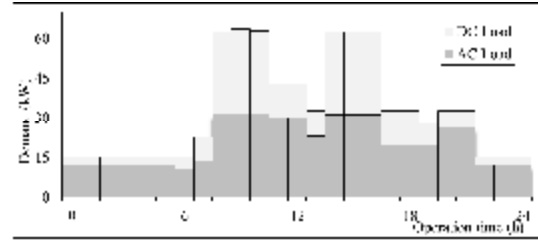


Fig. 3. The AC and DC share of the total electricity load.

Table 1. PHEVs' traffic data

| PHEV's no. | $t_{arr}$ (hr) | $t_{dep}$ (hr) | $SOC_{in}$ | $SOC_{out}$ |
|------------|----------------|----------------|------------|-------------|
| 1          | 7              | 20             | 0.8        | 0.8         |
| 2          | 8              | 18             | 0.2        | 1           |
| 3          | 8              | 17             | 0.5        | 0.9         |
| 4          | 9              | 14             | 0.8        | 0.3         |
| 5          | 9              | 17             | 0.4        | 1           |
| 6          | 9              | 17             | 0.35       | 0.9         |
| 7          | 9              | 18             | 0.5        | 0.9         |
| 8          | 10             | 18             | 0.7        | 0.7         |
| 9          | 10             | 19             | 0.85       | 0.3         |
| 10         | 11             | 20             | 0.4        | 0.9         |

The existing electricity resources of the case study are: 40 kW DG unit, 25 kW wind turbine and 25 kW PV arrays. Ten vehicles traffic to the parking lot with same battery storage capacity of 5 kWh. The considered arrival/departure time and the corresponding SOCs are listed in Table 1. Moreover, the described LN is connected to external grid to balance its shortage/extra power up to 20 kW. The additional required data is summarized in Table 2.

Table 2. Additional required data

| DG unit               |                             |
|-----------------------|-----------------------------|
| $h_{DG}$              | 0.35                        |
| $RR$                  | 20 (kW/h)                   |
| $C_{O\&M}$            | 0.03 (USD/h)                |
| $HR$                  | 10.78 (kWh/m <sup>3</sup> ) |
| Converter             |                             |
| $P_{conv}$            | 40 (kW)                     |
| $h_{AC/DC}$           | 0.90                        |
| $h_{DC/AC}$           | 0.85                        |
| PHEV's battery        |                             |
| $QEV^n$               | 5 (kWh)                     |
| $PEV^n_{charge,max}$  | 1.1 (kW)                    |
| $PEV^n_{dcharge,max}$ | 2.45 (kW)                   |
| $SOC^n_{min}$         | 0.20                        |

The price of natural gas is considered 0.328 USD/m<sup>3</sup> [16]. The selling price (spot price) and time-of-use rates are shown in Fig. 4 [16].

Table 3 shows the required data for investment analysis of hybrid and conventional LNs. The assumed cost of wiring is presented in ( $USD/m^2$ ) and is consisted of the cost wires, outlets, switches, labors, etc. Considering the investment cost and lifetime of each component, equation (31) represents the annualized cost of the components.

$$A = \left[ \frac{i_R (1 + i_R)^m}{(1 + i_R)^m - 1} \right] P \tag{31}$$

Where  $i$  is assumed to be 0.83 (%).

**5.2. Results and Discussions**

**a) Results of Operation Study**

The mentioned model is solved by GAMS software

**Table 3.** Required data for investment analysis

|                                   | Investment Cost | Lifetime (yr) | Annualized cost |
|-----------------------------------|-----------------|---------------|-----------------|
| Device Converter (\$/kW) [15]     | 655             | 15            | 46.62           |
| Inter-grid Converter (\$/kW) [15] | 700             | 15            | 49.83           |
| AC-DC Wiring (\$/m <sup>2</sup> ) | 25              | 20            | 1.36            |
| AC Wiring (\$/m <sup>2</sup> )    | 20              | 20            | 1.089           |

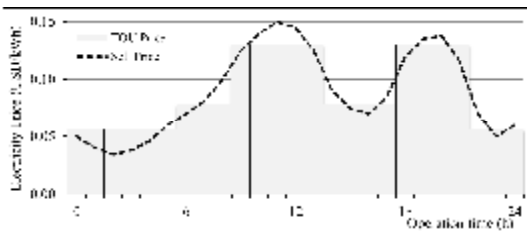


**Fig. 4.** The electricity exchange prices.

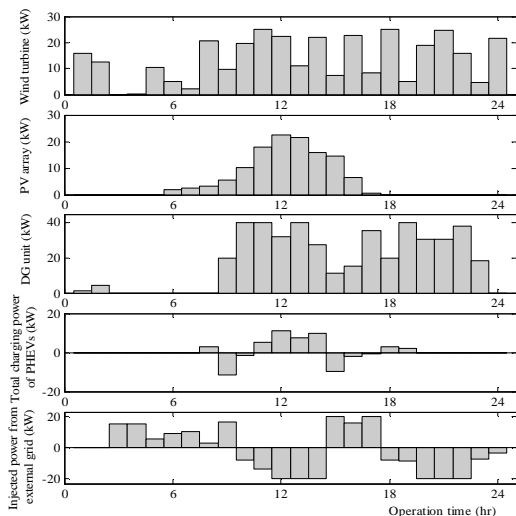


**Fig. 5.** Operation results of hybrid AC-DC LN.

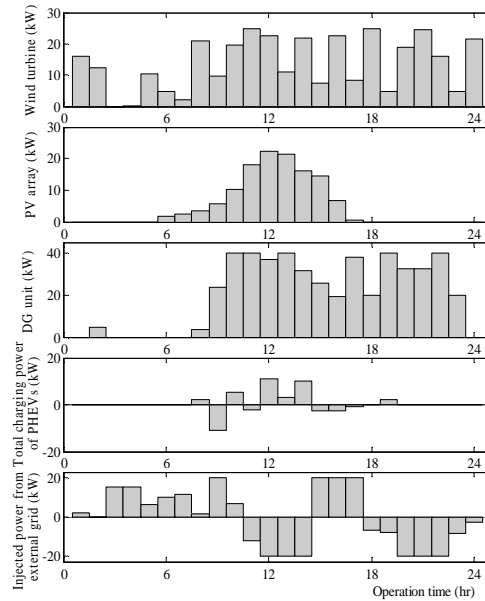


**Fig. 6.** Operation results of conventional AC LN.

using CPLEX solver. Figs. 5 and 6 illustrate the operation results of all LN’s resources; namely output power of wind turbine, PV arrays, diesel generator, total charging power of PHEVs and injected power from the external grid for hybrid AC-DC and conventional AC LN, respectively. As it can be figured out from the results of two LNs the output power of DG unit in both networks follows spot prices to decrease the total operation costs of the system. Moreover, in high spot price periods (10:00 – 14:00 and 18:00 – 22:00), the power is transferred from LN to the external grid and on the other hand, in low spot price period the power is transferred from external grid to LN due to economical optimization.

Fig.7 depicts the variation of the SOC level of PHEV’s batteries for hybrid AC-DC and conventional AC LN over the operation time. By focusing on Fig. 7, it can be seen that the number of various SOC levels is greater in hybrid AC-DC LN in compare with the conventional AC LN. Thus, PHEV’s batteries in hybrid AC-DC LN are utilized more effectively which play a vital role in reducing the intermittency of RERs.

The final results over operation time for both hybrid AC-DC LN and conventional AC LN are presented in Table 4. The total absorbed energy from the grid in hybrid AC-DC LN is decreased about 11.9 percent. Furthermore, total delivered energy to the grid in hybrid AC-DC LN is increased about 7.6 percent. It can be concluded that in the hybrid AC-DC LN, the flexibility of power exchange with the external grid and the opportunity of optimum utilization from the advantages of selling price variation is improved significantly.

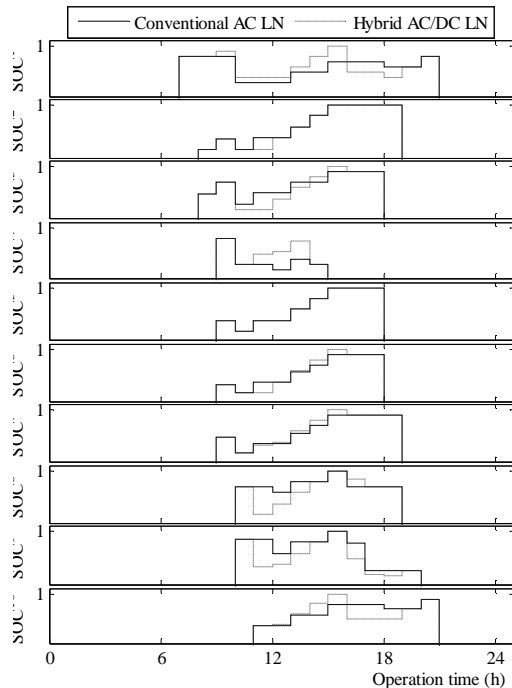


Fig. 7. SOC levels of both hybrid AC-DC LN and conventional AC LN.

Table 4. Final results of operation over 24 hours

|                                                 | Local Network Type |              |
|-------------------------------------------------|--------------------|--------------|
|                                                 | AC                 | Hybrid AC-DC |
| Total Absorbed Energy from Grid (kWh)           | 149.1              | 131.3        |
| Total Delivered Energy to Grid (kWh)            | 157.9              | 169.9        |
| Total Natural Gas Consumption (m <sup>3</sup> ) | 129.5              | 117.8        |
| Total operation cost (USD)                      | 29.97              | 22.84        |

The total natural gas consumption in hybrid AC-DC LN is decreased about 9 percent, due to two main reasons. First, in conventional AC LN the total load of the system is increased as a result of adding converters' losses as it was considered in Eq. 3. Second, batteries power exchange matches the generation of RERs with LN loads. Moreover, it can be noticed that the total operation cost in hybrid AC-DC LN is decreased about 23.8 percent.

b) Results of Investment Analysis

Since some components of hybrid and conventional LN are common, those are not considered in the investment analysis and the impacts of each LN's individual components are compared with each other. Wind turbine, PV array and battery generate DC power and should be connected to the AC bus via DC/AC converter. Thus, conventional AC LN requires three

device converters. However, these resources can be connected directly to the DC bus of hybrid AC-DC LN and the mentioned device converters are omitted. While an inter-grid converter must be added between the AC and DC sub-systems in the hybrid LN. As it was mentioned before, LNs are designed to service a four-story building with an area of about 2000 m<sup>2</sup>. The cost of wiring for both AC and AC-DC LNs are taken into account for the building.

For investment analysis of hybrid and conventional LNs, the annualized cost index is considered in this study with notice to different lifetimes of the components. As it is shown in table 5, the results show the annualized cost of hybrid AC-DC LN is about 17 percent lower than conventional AC LN. This index represents the economic viability of the hybrid LN.

c) Results of Reliability Assessment

Reliability assessment is simulated by DIGSILENT power factory software (version 14.0.504). The required data for running

Table 5. Final results of annualized cost analysis

|                       | Component (number or meter) | AC           | AC-DC  |
|-----------------------|-----------------------------|--------------|--------|
|                       |                             | Conventional | Hybrid |
| Device Converter      | 3×25 kW                     | 3496.5       | -      |
| Inter-grid Converter  | 1×40 kW                     | -            | 1993.2 |
| AC-DC Wiring          | 2000 m <sup>2</sup>         | -            | 2720   |
| AC Wiring             | 2000 m <sup>2</sup>         | 2178         | -      |
| Total annualized cost |                             | 5674.5       | 4713.2 |

Table 6. Final results of reliability assessment

|                | Local Network Type    |                       |
|----------------|-----------------------|-----------------------|
|                | Conventional AC       | Hybrid AC-DC          |
| EENS (kWh/day) | 1.617                 | 2.459                 |
| ASUI           | 10.6×10 <sup>-4</sup> | 16.3×10 <sup>-4</sup> |

reliability assessment for PV array, wind turbine and the converters are given in [17, 18] and other reliability data are extracted from the common global type of the components that exists in the library of DIGSILENT power factory. Table 6 addresses the results of reliability assessment by presenting the values of EENS and ASUI indices of conventional AC and hybrid LNs. As it can be seen in table 6, EENS index of hybrid AC-DC LN is increased about 52 percent in compare with conventional AC LN and its ASUI is increased about 54 percent. The reduction of overall reliability level of the hybrid LN was expected because the conventional AC LN was modeled in reliability

assessment as a single node model and all the resources and loads are connected through a single bus. While hybrid AC-DC LN's resources and loads are divided in two buses and an inter-grid inverter connect them together.

## 6. Conclusion

In this paper, two different topologies for local networks (LNs) with multi AC and DC resources; namely conventional AC and hybrid AC-DC LN and loads were presented. In conventional AC LN, all AC and DC resources (DG unit, wind turbine, PV array and PHEVs) and loads are connected to a single AC link with separate converters. An additional DC link exists in hybrid AC-DC LN that all DC resources and loads can be connected to it directly. Furthermore, a main converter provides the power transmission between AC and DC links in hybrid AC-DC LN. Since most of Renewable Energy Resources (RERs) produce DC power, hybrid AC-DC LNs will facilitate widespread use of these resources to meet emerging DC loads by reducing the intermittency of RERs through their integration with PHEVs. It can be concluded from the results of operation study that the operation cost can be reduced about 24 percent. The investment conducted and the annualized cost of hybrid LN is calculated 17 percent lower than conventional AC LN. On the other hand, the average system unreliability index of the hybrid LN is increased about 54 percent in compare with conventional AC LN.

## References

- [1] A. Ballatine, C. Pearson, R. Gurunathan, P. Pmsvsv, and A. Doronzo, "DC Micro-Grid," United States Patents Patent, 2012.
- [2] P. Wang, L. Goel, X. Liu, and F. H. Choo, "Harmonizing AC and DC: A Hybrid AC/DC Future Grid Solution," *IEEE Power and Energy Magazine*, vol. 11, pp. 76-83, 2013.
- [3] A. Milo, H. Gaztanaga, I. Etxeberria-Otadui, E. Bilbao, and P. Rodriguez, "Optimization of an experimental hybrid microgrid operation: reliability and economic issues," in *IEEE PowerTech*, Bucharest, 2009, pp. 1-6.
- [4] C. K. Ekman, "On the synergy between large electric vehicle fleet and high wind penetration—An analysis of the Danish case," *Renewable Energy*, vol. 36, pp. 546-553, 2011.
- [5] Q. Zhang, T. Tezuka, K. N. Ishihara, and B. C. Mclellan, "Integration of PV power into future low-carbon smart electricity systems with EV and HP in Kansai Area, Japan," *Renewable Energy*, vol. 44, pp. 99-108, 2012.
- [6] V. Gass, J. Schmidt, and E. Schmid, "Analysis of alternative policy instruments to promote electric vehicles in Austria," *Renewable Energy*, 2012.
- [7] D. B. Richardson, "Electric vehicles and the electric grid: A review of modeling approaches, Impacts, and renewable energy integration," *Renewable and Sustainable Energy Reviews*, vol. 19, pp. 247-254, 2013.
- [8] S. M. Borba, A. Szklo, and R. Schaeffer, "Plug-in hybrid electric vehicles as a way to maximize the integration of variable renewable energy in power systems: The case of wind generation in northeastern Brazil," *Energy*, vol. 37, pp. 469-481, 2012.
- [9] D. Dallinger and M. Wietschel, "Grid integration of intermittent renewable energy sources using price-responsive plug-in electric vehicles," *Renewable and Sustainable Energy Reviews*, vol. 16, pp. 3370-3382, 2012.
- [10] L. Xiong, W. Peng, and L. Pohchiang, "A hybrid AC/DC microgrid and its coordination control," *IEEE Trans. on Smart Grid*, vol. 2, pp. 278-286, 2011.
- [11] W. Peng, L. Xiong, J. Chi, L. Pohchiang, and C. Fookhoong, "A hybrid AC/DC micro-grid architecture, operation and control," in *IEEE Power and Energy Society General Meeting*, 2011, pp. 1-8.
- [12] A. A. A. Radwan and Y.-R. Mohamed, "Assessment and mitigation of interaction dynamics in hybrid AC/DC distribution generation systems," *IEEE Trans. on Smart Grid*, vol. 3, pp. 1382-1393, 2012.
- [13] K. Kurohane, T. Senjyu, A. Uehara, A. Yona, T. Funabashi, C.-H. Kim, "A hybrid smart AC/DC power system," in *5th IEEE Conference on Industrial Electronics and Applications (ICIEA)*, 2010, pp. 764-769.
- [14] J. Zhenhua and Y. Xunwei, "Hybrid DC- and AC-linked microgrids: towards integration of distributed energy resources," presented at the *IEEE Energy 2030 Conference*, 2008.
- [15] M. S. Ngan and C. W. Tan, "Assessment of economic viability for PV/wind/diesel hybrid energy system in southern Peninsular Malaysia," *Renewable and Sustainable Energy Reviews*, vol. 16, pp. 634-647, 2011.
- [16] X. Guan, Z. Xu, and Q.-S. Jia, "Energy-efficient buildings facilitated by microgrid," *IEEE Trans. on Smart Grid*, vol. 1, pp. 243-252, 2010.
- [17] L. Koh, G. Z. Yong, W. Peng, and K. Tseng, "Impact of Energy Storage and Variability of PV on Power System Reliability," *Energy Procedia*, vol. 33, pp. 302-310, 2013.

- [18] J. M. Pinar Pérez, F. P. García Márquez, A. Tobias, and M. Papaelias, "Wind turbine reliability analysis," *Renewable and Sustainable Energy Reviews*, vol. 23, pp. 463-472, 2013.